WATER RESOURCES RESEARCH, VOL. 25, NO. 10, PAGES 2159–2169, OCTOBER 1989

Density-Driven Flow of Gas in the Unsaturated Zone Due to the Evaporation of Volatile Organic Compounds

RONALD W. FALTA, IRAJ JAVANDEL, KARSTEN PRUESS, AND PAUL A. WITHERSPOON

Earth Sciences Division, Lawrence Berkeley Laboratory, University of California, Berkeley

A theoretical investigation of factors affecting the gas phase transport of evaporating organic liquids in the unsaturated zone is presented. Estimates of density-driven advective gas flow using a simple analytic expression indicate that significant advective gas flow will result from the evaporation of volatile liquids in soils having a high permeability. Numerical simulations using a two-dimensional cylindrical geometry and including the effects of phase partitioning between the solid, gas, water, and organic liquid phases show that mass transfer due to density-driven flow may dominate the gas phase transport of some organic chemical vapors in the unsaturated zone.

INTRODUCTION

At many sites in the United States and other countries, groundwater supplies are threatened by contamination from volatile organic compounds (VOC) such as solvents and hydrocarbon fuels. These contaminants may enter the ground as separate phase liquids due to chemical spills, chemical waste burials, or leaking storage tanks.

During the migration of these liquids through the unsaturated zone, a certain amount of the liquid will be retained in the soil by capillary forces. This trapped fraction is known as the residual saturation, and may occupy from about 2–20% of the available pore space [*Schwille*, 1984]. The fate of this trapped liquid in the unsaturated zone is determined by the degree of evaporation and transport in the gas phase, dissolution and transport in the aqueous phase, and chemical and biological reactions. Although the organic liquid may be trapped in the unsaturated zone above the water table, chemical transport in the gas and aqueous phases may result in contamination of the underlying groundwater.

In locations where the depth to the water table is large, and the amount of infiltration is small, gas phase chemical transport may be the dominant process by which the groundwater becomes contaminated. For example, groundwater beneath waste management facilities at Idaho National Engineering Laboratory is known to be contaminated with organic chemicals including carbon tetrachloride. The depth to the water table at this site is about 177 m. It has been postulated that the groundwater contamination by carbon tetrachloride is due to gas phase transport [*Hull*, 1988].

The determination of the extent and location of subsurface contamination is generally done by testing samples from monitoring wells or soil bores. This process is usually expensive and time consuming. Recently, soil gas analyses have been used as an alternative method for detecting and mapping the extent of subsurface contamination by VOCs [*Albertsen and Matthes*, 1978; *Wittman et al.*, 1985; *Marrin and Thompson*, 1987; *Thompson and Marrin*, 1987; *Devitt et al.*, 1987; *Marrin and Kerfoot*, 1988].

In order to evaluate the potential for groundwater contamination from residual saturations of VOC in the unsaturated zone, and to interpret the results of soil gas surveys, an understanding of the mechanisms of gas phase chemical transport is necessary. The transport of contaminants in the gas phase may occur due to both advection and diffusion and is influenced by phase partitioning into the water and solid phases. Gas phase advection may result from gas pressure or gas density gradients.

As organic liquids with high vapor pressures and molecular weights evaporate, the density of the gas in contact with the liquid changes with respect to the ambient soil gas. This density contrast results in an advective gas flow, the magnitude of which is dependent on the properties of the evaporating chemical and the porous medium. Under certain conditions, this density-driven gas flow may dominate the transport of contaminants in the gas phase.

Past studies involving porous medium density-driven flow have mainly addressed problems involving systems which are liquid saturated. These studies generally fall into two categories: salt water intrusion in coastal aquifers (see, for example, *Bear* [1979]), and thermally driven convection in geothermal systems or near high-level nuclear waste repositories (see, for example, *Bejan* [1984]). Recently, *Tsang and Pruess* [1987] conducted a study of thermally driven gas convection near a high-level nuclear waste repository. During the revision of the present paper, the results of a study conducted by *Sleep and Sykes* [1989] was published. They developed a two-dimensional finite element code to simulate the transport of VOCs in the unsaturated zone and included the effect of density driven flow in the gas phase. Their simulations of trichloroethylene (TCE) transport show the importance of including density-driven gas flow as a transport mechanism in the unsaturated zone. With the exception of the work of *Sleep and Sykes* [1989], present unsaturated zone contaminant transport modeling approaches consider gas diffusion to be the only means of contaminant transport in the gas phase [*Jury et al.*, 1983; *Swallow and Gschwend*, 1983; *Abriola*, 1984; *Baehr*, 1984; *Abriola and Pinder*, 1985*a*, *b*; *Baehr and Corapcioglu*, 1987; *Baehr*, 1987; *Silka*, 1988]. In this paper, we direct our attention to the relative importance of evaporation and density-driven flow in gas phase contaminant transport in the vadose zone.

Paper number 89WR01316.

TABLE 1. Thermodynamic Properties of Some Common Groundwater Contaminants

Chemical	Molecular Weight, M g/mole	Vapor Pressure, P^{0}* kPa (at 25°C)	Saturated Vapor Concentration, C_g^0† kg/m^3	Total Gas Density ρ_g^0,‡ kg/m^3
Trichloroethylene	131.4	9.9	0.52	1.58
Toluene	92.1	3.8	0.14	1.27
Benzene	78.1	12.7	0.40	1.42
Chloroform	119.4	25.6	1.23	2.11
Tetrachloroethylene	165.8	2.5	0.17	1.31
1,1,1-trichloroethane	133.4	16.5	0.89	1.87
Ethylbenzene	106.2	1.3	0.06	1.22
Xylene	106.2	1.2	0.05	1.21
Methylene chloride	84.9	58.4	2.00	2.50
1,2-dichloroethylene	96.9	43.5	1.70	2.37
1,2-dichloroethane	99.0	10.9	0.44	1.48
Chlorobenzene	112.6	1.6	0.07	1.23
1,1-dichloroethane	99.0	30.1	1.20	2.03
Carbon tetrachloride	153.8	15.1	0.94	1.93
Air at 1 atm, 25°C	28.6	(101.3)		1.17

*From *Devitt et al.* [1987].
†Calculated using (1).
‡Calculated using (2).

Estimation of Density-Driven Gas Velocities

In a natural convection system, fluid flow occurs due to variations in the density of the fluid in the system. These variations in density may be due to either temperature or concentration distributions in the fluid. As an organic liquid evaporates into the gas phase, the saturated vapor concentration may be calculated from the ideal gas law

$$C_g^0 = P^0 M/RT \tag{1}$$

where C_g^0 is the saturated vapor concentration of the VOC, P^0 is the saturated vapor pressure of the liquid VOC, M is the molecular weight of the liquid VOC, R is the universal gas constant, and T is the absolute temperature. For the range of pressures and temperatures usually encountered in the shallow subsurface environment, the use of (1) for real gases is not expected to lead to significant errors.

If the liquid is evaporating into air, the total gas phase density at equilibrium with the evaporating liquid, ρ_g^0, is

$$\rho_g^0 = \frac{P^0(M - M_{\text{air}}) + P_T M_{\text{air}}}{RT} \tag{2}$$

where M_{air} is the mixture molecular weight of air, and P_T is the total pressure. It should be noted that the mixture molecular weight of air depends on the humidity of the air. Dry air has a mixture molecular weight of 28.97 g/mole, while air saturated with water at a temperature of 25°C and a pressure of one atmosphere has a mixture molecular weight of 28.63 g/mole. The derivation of (2) is based on the assumption that the system obeys Dalton's law. The saturated vapor concentration and resulting total gas densities for several common volatile organic compounds are given in Table 1. These values were calculated at a temperature of 25°C and a total pressure of one atmosphere. Since the density of air under these conditions is 1.17 kg/m^3, it is clear from Table 1 that the evaporation of many organic liquids results in a gas phase density significantly larger than that of pure air.

By using an analysis based on *Hubbert*'s [1940] definition of fluid potential, it is possible to calculate the potential of a fluid of density ρ^0 where the ambient density is ρ_∞. By taking the derivative of this potential with respect to the vertical coordinate, and applying Darcy's law, one obtains

$$V_d = \frac{kg}{\mu}(\rho^0 - \rho_\infty) \tag{3}$$

where V_d is the darcy velocity, k is the permeability, g is the magnitude of gravitational acceleration, and μ is the fluid dynamic viscosity. This expression represents an order of magnitude estimate for the downward darcy velocity of a parcel of fluid of density ρ^0 through an otherwise stagnant fluid of density ρ_∞. This equation does not account for the effects of diffusion, phase partitioning, or boundaries on the fluid velocity.

Cheng and Minkowycz [1977] obtained an equivalent equation to (3) for the maximum convective velocity adjacent to a heated vertical flat plate embedded in a porous medium. *Bejan* [1984] shows that this expression also applies to the case where fluid density variations are caused by concentration variations in isothermal systems. For gas flow in the unsaturated zone, the ambient fluid is air, so $\rho_\infty = \rho_{\text{air}}$. In the vicinity of an evaporating VOC, the maximum gas density is given by (2). Combining (2) with the ideal gas law for the air density and neglecting any pressure gradients in the system gives

$$\rho_g^0 - \rho_{\text{air}} = \frac{P^0(M - M_{\text{air}})}{RT} \tag{4}$$

Writing (3) for the gas phase in a multiphase system,

$$V_d = \frac{kk_{rg}gP^0}{\mu_g RT}(M - M_{\text{air}}) \tag{5}$$

or

$$V_p = \frac{kk_{rg}gP^0}{\phi S_g \mu_g RT}(M - M_{\text{air}}) \tag{6}$$

where V_p is the pore velocity, ϕ is the porosity, μ_g is the gas viscosity, S_g is the gas phase saturation, and k_{rg} is the gas phase relative permeability.

TABLE 2. Estimate of Maximum Downward Gas Pore Velocities

Chemical	$\rho_g^0 - \rho_{air}$,* kg/m^3	Velocity,† m/day
Trichloroethylene	0.41	0.63
Toluene	0.10	0.15
Benzene	0.25	0.39
Chloroform	0.94	1.45
Tetrachloroethylene	0.14	0.22
1,1,1-trichloroethane	0.70	1.08
Ethylbenzene	0.05	0.08
Xylene	0.04	0.06
Methylene chloride	1.32	2.03
1,2-dichloroethylene	1.20	1.85
1,2-dichloroethane	0.31	0.48
Chlorobenzene	0.06	0.09
1,1-dichloroethane	0.86	1.33
Carbon tetrachloride	0.76	1.17

Assumptions: $kk_{rg} = 1 \times 10^{-11}$ m^2, $\mu_g = 1.83 \times 10^{-5}$ kg m^{-1} s^{-1}, $\phi = 0.4$, $S_g = 0.75$, $\rho_{air} = 1.17$ kg/m^3, and $T = 25$°C.
*Calculated using (4).
†Calculated using (6).

Depending on the molecular weight of the evaporating liquid, the density-driven gas flow may be upward or downward. If $M > M_{air}$, the flow will be downward; if $M < M_{air}$, the flow will be upward. In almost all cases, organic liquids have molecular weights which are greater than air so the resulting density-driven flows will usually be downward. The magnitude of the density-driven flow velocity varies linearly with the permeability, and density contrast, $\rho_g^0 - \rho_{air}$. Values of the pore velocities of several gases listed in Table 1 have been tabulated in Table 2. These values were calculated for an effective gas phase permeability (kk_{rg}) of 1×10^{-11} m^2 ($\approx$10 darcys), a viscosity of 1.83×10^{-5} kg/ms, a porosity of 0.4, and a gas saturation of 0.75. It should be emphasized that because (5) and (6) do not account for the effects of diffusion, phase partitioning, transient behavior, or geometrical influences on the density-driven flow velocity, the gas velocity calculated by these equations is an order of magnitude estimate of the maximum density-driven gas velocity. The magnitudes of the pore velocities given in Table 2 show that significant gas flows may occur in systems of high permeability.

In situations where the evaporation of VOCs is influenced by density-driven flow, it is possible to estimate the resulting rate of evaporation due to density-driven flow. If it is assumed that the density-driven gas flow through a region containing residual saturations of a VOC is uniform and vertical, and that the gas is in chemical equilibrium with the evaporating liquid, the rate of evaporation per unit horizontal cross-sectional area E may be calculated by multiplying (5) and (1):

$$E = V_d C_g^0 = \frac{kk_{rg} g}{\mu_g} \left(\frac{P^0}{RT}\right)^2 M(M - M_{air}) \quad (7)$$

From (7) it is apparent that the rate of evaporation due to density-driven flow is a linear function of gas permeability and a nonlinear function of the evaporating liquid vapor pressure and molecular weight. As with (5) and (6), (7) does not account for the effects of diffusion, water and solid phase partioning, transient behavior, or geometrical influences, and should be used with caution.

PHASE PARTITIONING

By assuming that local chemical equilibrium exists between the liquid VOC phase, the gas phase, the water phase, and the solid phase, relationships may be written which give the concentration of a compound in one phase in terms of the concentration in another phase. If it is further assumed that these relationships are linear, then the description of phase partitioning becomes straightforward.

The partitioning between water and gas is commonly described by Henry's law

$$C_g = HC_w \quad (8)$$

where C_g is the gas phase concentration of the VOC, C_w is the water phase concentration of the VOC, and H is Henry's constant for the VOC. Henry's constant for many compounds of low solubility may be calculated by

$$H = C_g^0/C_w^0 \quad (9)$$

where C_g^0 is the saturated vapor concentration of the chemical given by (1), and C_w^0 is the solubility of the chemical in water [*Jury et al.*, 1983]. If the liquid VOC phase is present, local equilibrium requires that $C_g = C_g^0$ and $C_w = C_w^0$.

If a similar relationship based on a linear adsorption isotherm is assumed to approximate the partitioning between the water and solid phases [*Freeze and Cherry*, 1979], then

$$\omega_s = K_D C_w \quad (10)$$

where ω_s is the mass fraction of the VOC adsorbed to the solid phase, C_w is the concentration of the VOC in the water, and K_D is the distribution coefficient for the chemical. Because the degree of adsorption of organic compounds depends largely on the amount of organic carbon present in the soil, K_D may be written as the product of the organic carbon partition coefficient, K_{oc}, and the organic carbon fraction in the soil, f_{oc} [*Karickhoff et al.*, 1979; *Schwartzenbach and Westfall*, 1981]:

$$K_D = K_{oc} f_{oc} \quad (11)$$

It is often more convenient to write (10) in terms of the adsorbed mass of the chemical per unit volume of soil C_s, in which case (10) becomes

$$C_s = \rho_b K_D C_w \quad (12)$$

where ρ_b is the dry bulk density of the soil. Values of K_{oc} for a number of organic compounds are available from *Jury et al.* [1984*b*] *and Karickhoff* [1981]. Several methods for estimating K_{oc} are summarized by *Lyman et al.* [1982].

The adsorbed concentration may be related to the gas phase concentration by combining (8) and (12):

$$C_s = \rho_b K_D C_g / H \quad (13)$$

Jury et al. [1983] and *Baehr* [1987] show that (8) and (13) may be used to derive a gas phase retardation coefficient:

$$R_g = \frac{S_w}{HS_g} + \frac{\rho_b K_D}{H\phi S_g} + 1 \quad (14)$$

This retardation coefficient is analogous to the standard water phase retardation coefficient and is equal to the ratio of the unretarded gas phase velocity to the actual gas phase chemical velocity retarded by aqueous and solid phase

TABLE 3. Gas Phase Retardation Coefficients for Several Organic Chemicals

Chemical	K_{oc}, m^3/kg	H	R_g	
			$f_{oc} = 0.001$	$f_{oc} = 0.005$
Benzene	0.083*	0.22*	4.4	10.4
Carbon tetrachloride	0.110*	0.94*	1.9	4.3
Chlorobenzene	0.150*	0.15*	8.2	28.2
Chloroform	0.029*	0.12*	5.0	9.8
Ethylene dibromide	0.044*	0.35*	2.6	5.1
Napthalene	1.300*	0.05*	137.7	657.7
n-octane	6.800*	140.0*	1.2	2.2
Phenol	0.027*	7×10^{-6}*	6.69×10^4	1.44×10^5
Toluene	0.140†	0.26†	5.0	14.5
1,1,1-trichloroethane	0.113‡	0.95†	1.9	4.3
Trichloroethylene	0.150‡	0.37†	3.9	12.0

Assumptions: $\phi = 0.4$, $S_g = 0.75\ S_w = 0.25$, and $\rho_b = 1500\ kg/m^3$.
**Jury et al.* [1984b].
†*Devitt et al.* [1987].
‡ *Josephson* [1983].

partitioning. Table 3 gives values of R_g for several organic compounds. These calculations were made for two values of f_{oc}, 0.001 and 0.005, with $\phi = 0.4$, $S_g = 0.75$, $S_w = 0.25$, and $\rho_b = 1500\ kg/m^3$. From this table, it is obvious that some compounds are very strongly retarded in the gas phase. Since phase partitioning from the gas phase into the water and solid phase diminishes the driving force for density-driven flow, compounds having very high retardation coefficients will not be strongly affected by density-driven flow. It is important to recognize that R_g for a given chemical may vary by over an order of magnitude depending on f_{oc}, S_w, S_g, ϕ, and ρ_b.

Numerical Simulator

In order to simulate the evaporation of organic liquids and transient density-driven flow, an existing code, TOUGH (Transport Of Unsaturated Groundwater and Heat), was modified. TOUGH, developed by *Pruess* [1987], is a three-dimensional numerical code for simulating the coupled transport of water, water vapor, air, and heat in porous and fractured media. The nonlinear, coupled, mass and heat balance equations are discretized spatially using the integral finite difference method [*Narasimhan and Witherspoon*, 1976]. Because of the strong nonlinearity and coupling of the governing equations, a completely simultaneous solution is performed. A detailed technical description of TOUGH may be found in the user's guide [*Pruess*, 1987]. TOUGH has been verified by comparison with several geothermal reservoir and unsaturated flow solutions [*Pruess and Wang*, 1984; *Pruess*, 1987].

The modified version of TOUGH used in the present application, which will be referred to as TOUGH VOC, simulates the coupled transport of a volatile organic compound (VOC) in the liquid and gas phases, and the transport of air. Both the gas phase and the liquid VOC phase are mobile. An immobile water phase is included, and the VOC is partitioned between the liquid VOC phase, the gas phase, the water phase, and the solid phase by assuming local chemical equilibrium between the phases.

The mass balance equations used in TOUGH VOC are

$$\frac{d}{dt}\int_V M^{(K)}\,dV = \int_\Gamma \mathbf{F}^{(K)} \cdot \mathbf{n}\,d\Gamma + \int_V q^{(K)}\,dV \quad (15)$$

$K = 1$ VOC $K = 2$ air

The mass accumulation term for the VOC is

$$M^{(1)} = \phi S_g \rho_g \omega_g^{(1)} + \phi S_L \rho_L \omega_L^{(1)} + \frac{\phi S_w \rho_g \omega_g^{(1)}}{H} + \frac{\rho_b \rho_g \omega_g^{(1)} K_D}{H} \quad (16)$$

where S_g is the gas saturation, S_L is the liquid VOC saturation, S_w is the water saturation, $\omega_g^{(1)}$ is the mass fraction of the VOC in the gas phase, $\omega_L^{(1)}$ is the mass fraction of the VOC in the liquid VOC phase (≈ 1), ρ_g is the gas phase density, and ρ_L is the liquid VOC phase density. The air mass accumulation term is

$$M^{(2)} = \phi S_g \rho_g \omega_g^{(2)} + \phi S_L \rho_L \omega_L^{(2)} \quad (17)$$

where $\omega_g^{(2)}$ is the mass fraction of air in the gas phase, and $\omega_L^{(2)}$ is the mass fraction of air in the liquid VOC phase. In general, $\omega_L^{(2)} \approx 0$. Partitioning of air into the water and solid phases is neglected.

Water is assumed to be immobile and to exist only as a liquid phase. For these reasons, a separate mass balance equation for the water is not required.

The mass flux terms sum over the liquid VOC phase and the gas phase

$$\mathbf{F}^{(K)} = \sum_\beta \mathbf{F}_\beta^{(K)} \quad (18)$$

β = liquid VOC, gas

The flux in each phase is

$$\mathbf{F}_\beta^{(K)} = \frac{-kk_{r\beta}\rho_\beta}{\mu_\beta}\omega_\beta^{(K)}(\nabla P_\beta - \rho_\beta \mathbf{g}) - \delta_{\beta g}\phi S_\beta \tau D_g \rho_\beta \nabla \omega_\beta^{(K)} \quad (19)$$

where k is the absolute permeability, $k_{r\beta}$ is the β phase relative permeability, μ_β is the β phase dynamic viscosity, P_β is the pressure in phase β, g is the gravitational acceleration vector, and D_g is the molecular diffusion coefficient of vapor in air. The second term on the right-hand side of (19) represents binary diffusion and only applies to the gas phase. The total gas phase diffusive mass flux summed over the VOC and air components is zero. Therefore the total gas phase mass flux is the product of the gas phase darcy velocity and the total gas phase density. The gas phase tortuosity τ is calculated from the *Millington and Quirk* [1961] model

$$\tau = \phi^{1/3} S_g^{7/3} \tag{20}$$

The gas phase is assumed to behave as an ideal gas, and additivity of partial pressures is assumed for air and VOC vapor.

The accuracy of TOUGH VOC was verified by comparison with an analytical solution for one-dimensional, transient gas diffusion with phase partitioning given by *Baehr* [1987]. The partial differential equation for one-dimensional transient gas diffusion with phase partitioning is

$$\frac{\partial C_g}{\partial t} = \frac{D_g}{R_g} \tau \frac{\partial^2 C_g}{\partial x^2} \tag{21}$$

where R_g is the gas phase retardation factor given by (14). Taking the boundary condition for the semi-infinite case as $C_g = C_{g0}$ at $x = 0$, and the initial condition as $C_g = 0$ at $t = 0$, the solution is [*Baehr*, 1987]

$$\frac{C_g}{C_{g0}} = \operatorname{erfc}\left(\frac{1}{2(\tau D_g/R_g)^{1/2}} \frac{x}{\sqrt{t}}\right) \tag{22}$$

In Figure 1, the results of a TOUGH VOC simulation are compared with the analytical solution, (22). In this case, $\phi = 0.4$, $S_g = 0.75$, $S_w = 0.25$, $H = 0.329$, $\rho_b = 1500$ kg/m^3, $K_D = 8.3 \times 10^{-4}$ m^3/kg, $D_g = 1.0 \times 10^{-5}$ m^2/s, and the time is 216.2 days. The values of H and K_D are representative of chemicals which are strongly adsorbed onto the solid phase and partitioned into the water phase. A numerical model with a total of 200 elements was used with a mesh spacing of 0.05 m from $x = 0$ to 5 m, and 0.4 m from $x = 5$ to 45 m. For the time period used in this example, the model was large enough to be considered as infinite in length, and the concentration was set to zero at the outer boundary. A total of 50 time steps was used with an initial time step of 10 s. The size of the time step was doubled after each time step. The comparison on Figure 1 shows a good match between the analytical and numerical solutions for transient diffusion.

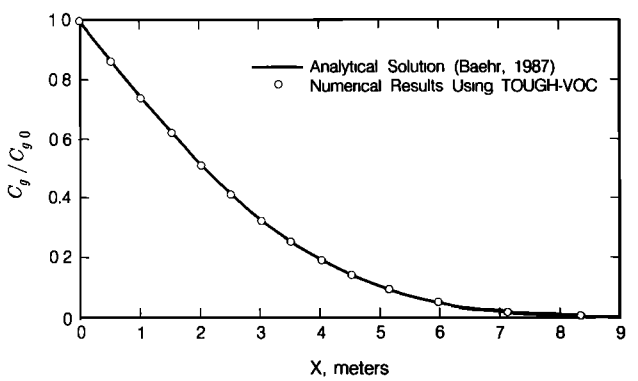

Fig. 1. Comparison of TOUGH VOC with analytical solution for transient diffusion with phase partitioning.

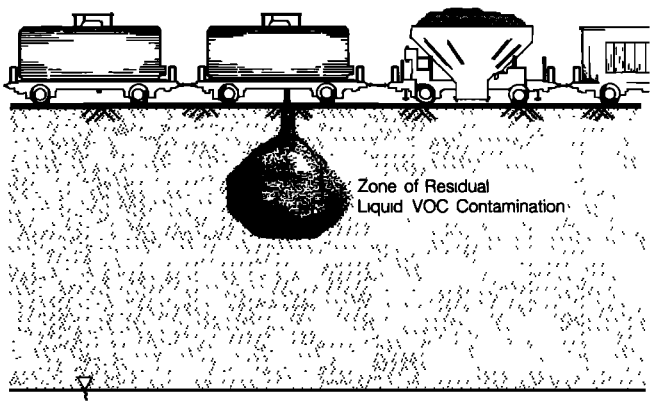

Fig. 2. Schematic diagram of the system to be modeled.

NUMERICAL SIMULATIONS

In order to better understand how evaporation and gas phase transport of VOCs occur in natural systems, a series of two-dimensional radially symmetric simulations were performed. A conceptual diagram of the system to be modeled is shown in Figure 2. In this figure, a liquid VOC has been released into the subsurface by a spill from a chemical tank car. Similar releases of organic liquids could occur from leaking underground storage tanks, industrial accidents, or the improper disposal of organic liquid wastes. It is assumed that the volume of this spill was large enough so that a significant volume of soil has become contaminated, but not so large that the liquid has migrated down to the water table. Within this contaminated volume of soil, the organic liquid is present at some residual saturation.

This system is modeled using the numerical simulator, TOUGH VOC. For the purpose of isolating the importance of certain parameters on the gas phase transport of a VOC, several simplifying assumptions are made. The unsaturated porous medium is assumed to be homogeneous and isotropic and to contain a uniform water saturation and a certain fraction of organic carbon. The system is assumed to be isothermal with no water infiltration from the ground surface. The gas phase relative permeability k_{rg} is taken to be S_g^3. This is similar to the gas phase relative permeability function given by *Fatt and Klikoff* [1959]. The liquid VOC phase is assumed to be immobile ($k_{rL} = 0$) as is the water phase. It is assumed that diffusion of the VOC through the water phase is negligible compared to diffusion of the VOC in the gas phase and that the gas phase viscosity is constant, and not a function of composition.

Gas viscosity is, in general, a function of composition. The viscosity of a multicomponent gas may be calculated as a function of composition by using the Lucas corresponding states method [*Reid et al.*, 1987]. Carrying out the calculations for dry air saturated with carbon tetrachloride vapor at 25°C and one atmosphere, we find that the viscosity is 1.72×10^{-5} kg/ms. Since the viscosity of dry air at this temperature is about 1.83×10^{-5} kg/ms, the variation of viscosity with

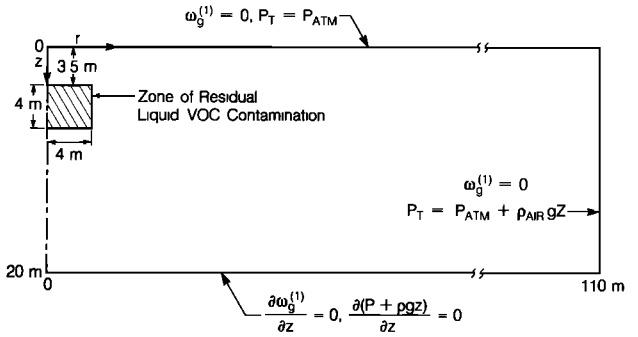

Fig. 3. Geometry and boundary conditions for numerical simulations considering density-driven flow.

composition in this case is fairly small. In cases where the evaporating liquid has a very high vapor pressure, the variation of viscosity with composition could be important. Partitioning of the VOC between the liquid VOC, water, gas, and solid phases is calculated according to local chemical equilibrium.

To illustrate the effect of density-driven gas flow on gas phase transport, two types of two-dimensional (r-z) simulations were performed, one in which transport occurs due to evaporation, diffusion, and density-driven flow, and one in which gravitational effects are suppressed by setting $\mathbf{g} = 0$ in (19).

The problem geometry and boundary conditions for the cases in which density-driven flow is considered are shown in Figure 3. At the ground surface, $z = 0$, the mass fraction of VOC in the gas phase is zero, $\omega_g^{(1)} = 0$. This implies that the concentration boundary layer above the ground surface has a thickness of zero and results in a maximum rate of mass transfer to the atmosphere by diffusion [*Jury et al.*, 1984*a*]. The pressure at the ground surface is held at atmospheric pressure (101.325 kPa). The water table, located 20 m below the ground surface, is assumed to be a no-flow boundary, i.e., $\partial \omega_g^{(1)}/\partial z = 0$; $\partial (P + \rho_g gz)/\partial z = 0$. In reality, there will be some mass transfer of VOC across the water table by diffusion in the water phase. The outer radial boundary is located at a radius of 50 m in the simulations where density-driven flow is neglected and at a radius of 110 m in the simulations where density-driven flow is included. In each simulation, the distance to the outer boundary is large enough to approximate a radially infinite system. At the outer boundary, the mass fraction of VOC in the gas phase is zero, $\omega_g^{(1)} = 0$, and the pressure is at static equilibrium, $P = P_{atm} + \rho_{air} gz$.

Initially, the liquid VOC occupies a cylindrical region centered at $r = 0$ with a radius of 4 m, a thickness of 4 m, and a saturation (S_L) of 0.1. For a porosity of 0.4, this corresponds to a liquid VOC volume of 8.042 m^3. The depth from the ground surface to the top of the contaminated zone is 3.5 m. The initial condition on the VOC mass fraction in the gas phase is $\omega_g^{(1)} = 0$ everywhere except in the region occupied by the liquid VOC where the mass fraction in the gas phase is determined by chemical equilibrium with the liquid VOC. The initial pressure distribution reflects the static equilibrium of air, $P = P_{atm} + \rho_{air} gz$.

The boundary and initial conditions for the simulations in which density-driven flow is not considered are similar to those described above except that the pressure at the outer radial boundary is atmospheric, $\partial P/\partial z = 0$ at the lower boundary, and the initial pressure is atmospheric everywhere.

Several initial simulations were conducted using a coarse grid spacing. The mesh was successively refined until the computed solution was no longer a significant function of the grid spacing. The computational grid spacing in the z direction is 1 m. In the radial direction, the grid spacing is 1 m from $r = 0$ to $r = 18$ m, 2 m from $r = 18$ m to $r = 38$ m, 3 m from $r = 38$ m to $r = 50$ m, 4 m from $r = 50$ m to $r = 74$ m, and 6 m from $r = 74$ m to $r = 110$ m. For the simulations in which the outer boundary is at a radius of 50 m, the outer part of the mesh is eliminated. The initial time step size in all of the simulations is 5000 s. The time step size is allowed to double after each time step to a maximum size of 1.8×10^6 s. The use of smaller time steps does not change the results appreciably. Additional problem specifications for the simulations are listed in Table 4. Simulations were performed for two different compounds, carbon tetrachloride and toluene. The carbon tetrachloride and toluene saturated vapor pressures listed in Table 4 are for a temperature of 20°C. These saturated vapor pressures correspond to saturated carbon tetrachloride and toluene gas concentrations of 0.7664 kg/m^3 and 0.1095 kg/m^3, respectively. The gas phase retardation coefficients of carbon tetrachloride and toluene for the conditions specified in the simulations are 1.9 and 5.0, respectively.

In Figures 4*a* and 4*b* the gas concentration distributions of carbon tetrachloride after 1 year without density-driven flow, and with density-driven flow are shown. Due to the relatively low permeability, $k = 1 \times 10^{-13}$ m^2, the contribution of density-driven advection to the overall gas trans-

TABLE 4. Problem Specification

Parameter	Value
Air diffusion constant	$D_g = 1 \times 10^{-5}$ m^2/s
Porosity	$\phi = 0.4$
Water saturation	$S_w = 0.25$
Initial liquid VOC saturation in contaminated zone	$S_L = 0.1$
Initial gas saturation in contaminated zone	$S_g = 0.65$
Fraction of organic carbon	$f_{oc} = 0.001$
Soil dry bulk density	$\rho_b = 1500$ kg/m^3
Gas viscosity	$\mu_g = 1.81 \times 10^{-5}$ kg m^{-1}s^{-1}
Gas relative permeability	$k_{rg} = S_g^3$
Temperature	$T = 20$°C
Saturated vapor pressure	
carbon tetrachloride	$P° = 12{,}130$ Pa
toluene	$P° = 2{,}900$ Pa
Molecular weight	
carbon tetrachloride	$M = 154$ g/mole
toluene	$M = 92$ g/mole
Liquid density	
carbon tetrachloride	$\rho_L = 1{,}584$ kg/m^3
toluene	$\rho_L = 862$ kg/m^3
Organic carbon partition coefficient	
carbon tetrachloride	$K_{oc} = 0.11$ m^3/kg
toluene	$K_{oc} = 0.14$ m^3/kg
Henry's constant	
carbon tetrachloride	$H = 0.958$
toluene	$H = 0.260$
Air density at 1 atm, 20°C	$\rho_{air} = 1.19$ kg/m^3

port in Figure 4*b* is minimal, and the concentration distributions with and without the density-driven flow are nearly identical. In this case, the use of a standard diffusion model to describe the gas phase transport would be appropriate.

Figure 5 shows a series of carbon tetrachloride gas concentration distributions after 1 year for permeabilities of 1×10^{-12}, 1×10^{-11}, and 3×10^{-11} m^2. These simulations, which include the effects of density-driven advection, illustrate the effect of permeability on gas phase mass transfer. It should be noted that the actual gas phase permeabilities in these simulations are somewhat lower than the media permeabilities because of the gas phase relative permeability which varies from 0.275 at a gas saturation of 0.65 to 0.422 at a gas saturation of 0.75. For a permeability of 1×10^{-12} m^2, the concentration distribution is somewhat different from those shown in Figures 4*a* and 4*b*. However, the effect of density-driven flow on the gas transport is still relatively small. As the permeability is increased to 1×10^{-11} m^2, and then to 3×10^{-11} m^2, the effect that the density-driven flow has on transport begins to become more significant. Directly above the zone of residual contamination, the concentration gradient increases with the permeability, a direct result of the downward flow of air through the liquid VOC contaminated zone. The upward diffusion of VOC vapors toward the ground surface is countered by this downward flow. Due to the influx of relatively clean air through the top of the liquid contaminated zone, the rate of evaporation of the VOC in this area increases with increasing permeability. Below the liquid chemical source, high carbon tetrachloride concentrations are found near the water table. As the dense, contaminated gas approaches the location of the water table, it tends to flow out radially along the water table.

In Figures 6*a* and 6*b*, the carbon tetrachloride distributions without and with density-driven flow for a permeability of 6×10^{-11} m^2 are compared. Although this is a high

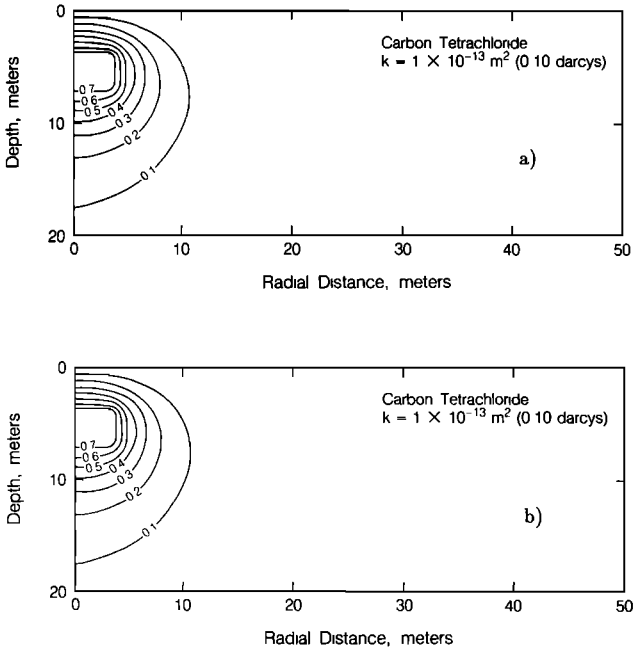

Fig. 4. Carbon tetrachloride gas concentration distributions (kilograms per cubic meter) after 1 year as a result of (*a*) evaporation and diffusion and (*b*) evaporation, diffusion, and density-driven flow.

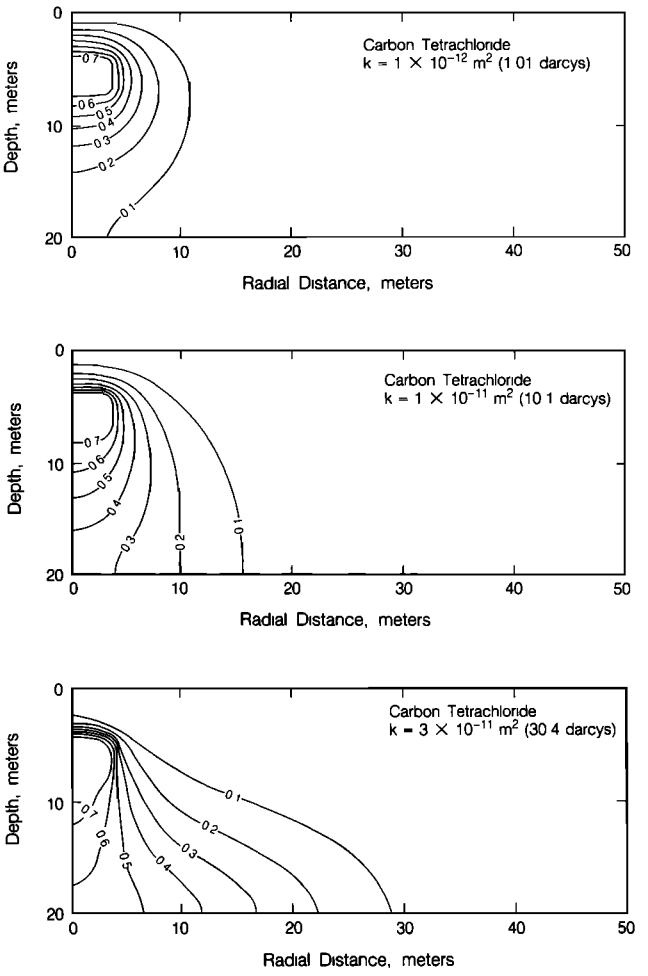

Fig. 5. Carbon tetrachloride gas concentration distributions (kilograms per cubic meter) after 1 year as a result of evaporation, diffusion, and density-driven flow for permeabilities of 1×10^{-12}, 1×10^{-11}, and 3×10^{-11} m^2.

permeability for natural systems, it is not uncommon for sand and gravel sediments. This comparison illustrates the dramatic effect that density-driven flow has on the gas phase transport of dense vapors in systems having high permeabilities. The assumption that diffusion alone determines the gas phase transport in this case would result in a misleading prediction of the contaminant transport.

From the preceeding examples, it might appear that the use of a diffusive model to describe the gas transport of VOCs in high-permeability systems is inappropriate. This is not necessarily true because the magnitude of density-driven flow effects depends on the chemical's saturated vapor density, and the degree to which the chemical is partitioned from the gas phase into the water and solid phases (see Tables 2 and 3). In Figures 7*a* and 7*b*, the results of simulations of the evaporation of toluene are shown. The permeability used in these simulations is large, 3×10^{-11} m^2, yet the difference between the case shown in Figure 7*a* which does not consider density-driven flow, and the one shown in Figure 7*b* which does consider density-driven flow, is not that great. There are two reasons for this. First, the saturated vapor density of toluene is fairly low, 0.1095 kg/m^3, resulting in a relatively small driving force for density driven flow. Second, due to the relatively low Henry's

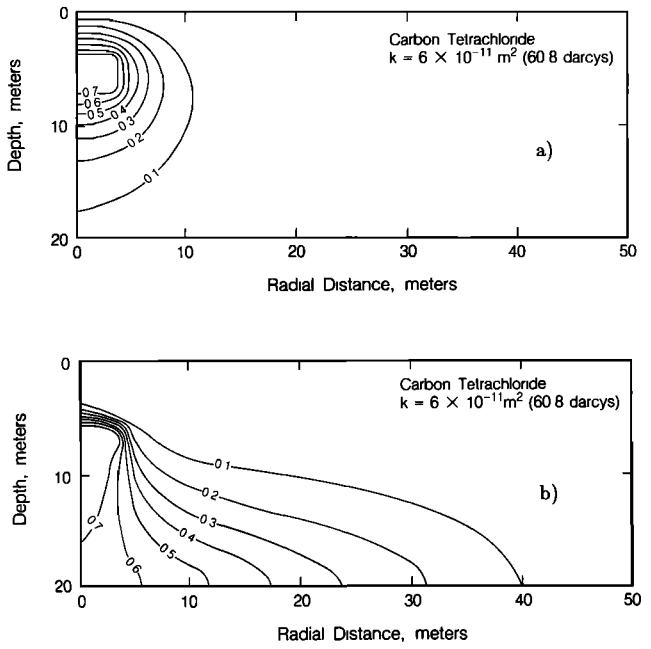

Fig. 6. Carbon tetrachloride gas concentration distributions (kilograms per cubic meter) after 1 year as a result of (*a*) evaporation and diffusion and (*b*) evaporation, diffusion, and density-driven flow.

constant for toluene, there is a strong partitioning of toluene from the gas phase into the water phase, resulting in a reduction of the driving force for density-driven flow.

The rate at which a liquid VOC evaporates from the unsaturated zone strongly depends on the magnitude of the density-driven gas flow velocity. A tabulation of the amount of liquid VOC removed from the unsaturated zone after 1 year of evaporation for the given examples is shown in Table

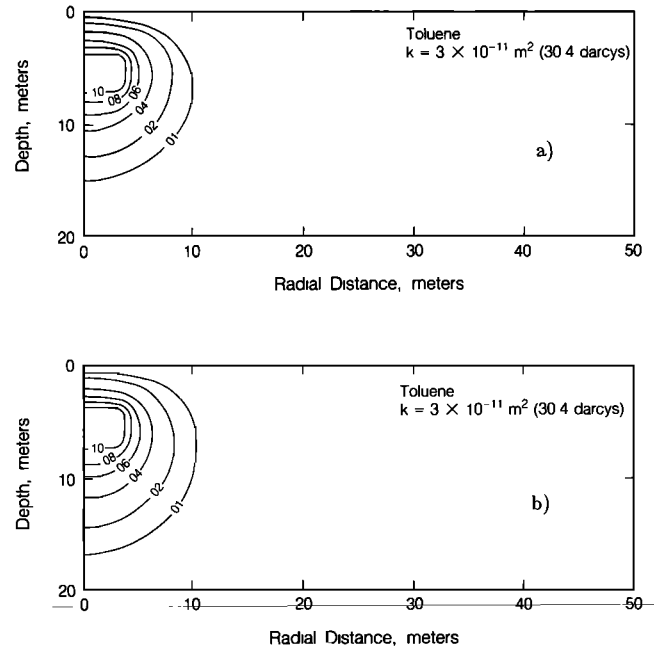

Fig. 7. Toluene gas concentration distributions (kilograms per cubic meter) after 1 year as a result of (*a*) evaporation and diffusion and (*b*) evaporation, diffusion, and density-driven flow.

TABLE 5. Fraction of Initial Liquid VOC Mass Removed After 1 Year

Chemical	Soil Permeability, m^2	Percent Removed	
		Diffusion only	Diffusion and Density-Driven Flow
Carbon tetrachloride	6×10^{-11}	15.1	59.2
	3×10^{-11}	15.1	35.3
	1×10^{-11}	15.1	19.2
	1×10^{-12}	15.1	15.2
	1×10^{-13}	15.1	15.1
Toluene	3×10^{-11}	4.0	4.2

5. In cases where the density-driven flow is considered and the permeability is large, the amount of carbon tetrachloride which has evaporated after 1 year is much larger than in the cases where the density-driven flow is neglected. In particular, when the permeability is 6×10^{-11} m^2, the amount of carbon tetrachloride which has evaporated considering density-driven flow and diffusion in almost 4 times larger than the amount which has evaporated considering only diffusion. For a given compound, this difference decreases with decreasing permeability. The effect of density-driven flow on the rate of toluene evaporation is small, even in the case of large soil permeabilities.

The transient gas velocity fields calculated in the simulations are complex functions of gas density gradients, gas phase permeability, diffusion, phase partitioning, and geometry. Within the zone of liquid VOC residual contamination, however, it is possible to make an order of magnitude estimate of the downward velocity using (6). This is possible only if the water table is located far enough below the evaporating liquid so that the gas velocity through the contaminated zone is not strongly affected by the lower boundary, and is primarily vertical. Owing to the assumption of local chemical equilibrium, the concentration of VOC in the gas phase is uniform and constant in regions containing separate phase liquids. This has the effect of reducing the influence of phase partitioning and diffusion on the gas velocity field within the zone. A comparison of estimated and simulated gas velocities in the region containing residual VOC saturations is given in Table 6. The estimated velocities were calculated using (6), with an assumed gas saturation of 0.65. This gas saturation corresponds to the initial gas saturation in the zone of residual VOC contamination (see Table 4). As in the numerical simulations, the gas phase

TABLE 6. Comparison of Estimated and Computed Vertical Gas Velocities in the Zone of Residual VOC Contamination After 1 Year

Chemical	Soil Permeability, m^2	Vertical Pore Velocity, m/s	
		Estimated*	Simulation
Carbon tetrachloride	6×10^{-11}	2.14×10^{-5}	1.81×10^{-5}
	3×10^{-11}	1.07×10^{-5}	9.50×10^{-6}
	1×10^{-11}	3.57×10^{-6}	2.98×10^{-6}
	1×10^{-12}	3.57×10^{-7}	2.69×10^{-7}
	1×10^{-13}	3.57×10^{-8}	3.45×10^{-8}
Toluene	3×10^{-11}	1.31×10^{-6}	9.68×10^{-7}

*Calculated using (6) with $\phi = 0.4$, $S_g = 0.65$, $\mu_g = 1.81 \times 10^{-5}$ kg $m^{-1}s^{-1}$, $g = 9.806$ m/s^2, $k_{rg} = 0.275$, and $T = 20$°C.

TABLE 7. Comparison of Estimated and Computed VOC Evaporation Due to the Density Driven Flow Alone

Chemical	Soil Permeability, m^2	Percent Removed	
		Estimated*	Simulation†
Carbon tetrachloride	6×10^{-11}	53.1	44.1
	3×10^{-11}	26.5	20.2
	1×10^{-11}	8.8	4.1
	1×10^{-12}	0.9	0.1
	1×10^{-13}	0.1	0.0
Toluene	3×10^{-11}	0.9	0.2

*Calculated using (7) with $\phi = 0.4$, $S_g = 0.65$, $\mu_g = 1.81 \times 10^5$ kg $m^{-1}s^{-1}$, $g = 9.806$ m/s^2, $k_{rg} = 0.275$, and $T = 20$°C. The horizontal cross-sectional area of the zone of residual VOC contamination is 50.3 m^2.

†Approximated by subtracting the percent removed by diffusion only from the percent removed by diffusion and density driven flow in Table 5.

relative permeability is taken to be S_g^3. The estimated values show a reasonable agreement with the computed values despite the many simplifying assumptions required by (6).

In Table 7 the estimated and numerically computed amounts of VOC evaporation after 1 year due to density-driven flow are compared. The estimated amount of VOC evaporation due to density-driven flow was calculated using (7) with an assumed gas saturation of 0.65 and a horizontal cross-sectional area of 50.3 m^2. It is not possible to completely isolate the effect of density-driven flow from the effect of diffusion on the amount of VOC evaporation in the numerical simulations. This is due to the interdependence between diffusion and density-driven flow. However, the amount of VOC evaporation due to density-driven flow in the simulations may be approximated by subtracting the amount of evaporation in the cases considering only diffusion from the amount of evaporation in the cases considering diffusion and density-driven flow (these quantities are tabulated in Table 5). The values of the amount of evaporation in the simulation column in Table 7 were calculated in this manner. The estimated and numerically simulated amounts of evaporation due to density-driven flow given in Table 7 are fairly close even though many simplifying assumptions were used in the derivation of (7). From Tables 6 and 7, it appears that the use of simple gas velocity and VOC density-driven evaporation estimates given by (6) and (7), in conjunction with the gas phase retardation coefficient, given by (14), may provide some insight as to whether or not density-driven flow is important for a given problem.

CONCLUSIONS

The results of this study indicate that under certain conditions density-driven gas flows in the unsaturated zone will occur during the evaporation of volatile organic liquids. The magnitude of these flows is mainly a function of the organic liquid saturated vapor pressure and molecular weight, the gas phase permeability, and the gas phase retardation coefficient. The potential for density-driven flow in a partially saturated system may be roughly estimated using a form of Darcy's law together with the retardation coefficient for a chemical in the system. Some common contaminants which are likely to be affected by density-driven flow include tricholorethylene, chloroform, 1,1,1-trichloroethane, methylene chloride, 1,2-dichloroethylene, 1,2-dichloroethane, 1-1-dichloroethane, carbon tetrachloride, Freon 113, and possibly, benzene. Some common contaminants which are not likely to be affected by density-driven flow include toluene, ethylbenzene, xylenes, chlorobenzene, napthalene, and phenols. In order for this gas flow to be significant, the gas phase permeability (in a homogeneous porous medium) should be at least on the order of 1×10^{-11} m^2 (≈10 darcy). The general direction of density-driven flow is downward from the evaporating source toward the water table, and radially outward along the water table.

The rate of evaporation of organic liquids from the unsaturated zone is a strong function of the strength of density-driven gas flow. The amount of the evaporation due to density-driven flow may be estimated by means of a simple analytic expression.

In this initial study, several simplifying assumptions have been made. It is suggested that future studies include the effect of soil heterogeneity and anisotropy on gas transport. It is likely that large-scale heterogeneities such as fractures, bedding, clay lenses, and buried stream channels will largely control the movement of evaporating vapors.

While the present study focused on single-component organic liquids, many groundwater pollution problems involve multicomponent organic liquids such as gasoline. Although numerical simulators have been developed which can simulate multicomponent effects, these models assume that the velocity field is uncoupled from the multicomponent concentration field. As shown in this paper, this assumption is not always reasonable.

Last, due to the low viscosity of gases, flows may occur in response to very small pressure gradients. An evaluation of the effects of variable pressure boundary conditions on gas phase transport would be of interest.

NOTATION

C_g concentration of VOC in the gas phase, kg/m^3.
C_s concentration of VOC in the solid phase, kg/m^3.
C_w concentration of VOC in the water phase, kg/m^3.
C_g^0 saturated VOC vapor concentration, kg/m^3.
C_w^0 solubility of VOC in water, kg/m^3.
D_g molecular diffusivity of VOC in air, m^2/s.
E VOC evaporation rate per unit horizontal cross-sectional area, kg/m^{2}s.
$\mathbf{F}_\beta^{(K)}$ mass flux of component K in the β phase, kg/m^{2}s.
f_{oc} fraction of organic carbon in the soil.
g magnitude of gravitational acceleration, m/s^2.
$\mathbf{g}$ gravitational acceleration vector, m/s^2.
H Henry's constant for air-water partioning of a VOC.
K_D VOC solid distribution coefficient, m^3/kg.
K_{oc} VOC organic carbon partition coefficient, m^3/kg.
k porous media permeability, m^2.
k_{rg} gas phase relative permeability.
k_{rL} liquid VOC phase relative permeability.
$k_{r\beta}$ β phase relative permeability.
M molecular weight of the VOC, g/mole.
M_{air} mixture molecular weight of air, g/mole.
$M^{(K)}$ mass of component K per unit porous medium volume, kg/m^3.
$\mathbf{n}$ unit normal vector.
P reference phase pressure, Pa.

P_{atm} atmospheric pressure, Pa.
P_T total pressure, Pa.
P_β β phase pressure, Pa.
P^0 saturated VOC vapor pressure, Pa.
$q^{(K)}$ rate of generation of component K per unit volume, kg/m^{3}s.
R universal gas constant, mJ/mole^{0}K.
R_g gas phase retardation coefficient.
S_g gas phase saturation.
S_L liquid VOC phase saturation.
S_w water phase saturation.
S_β β phase saturation.
T temperature, °K.
V volume of porous medium, m^3.
V_d darcy velocity, m/s.
V_P pore velocity, m/s.
Γ surface area, m^2.
$\delta_{\beta g}$ Kronecker delta (=1 for $\beta = g$, =0 otherwise).
μ_g gas phase viscosity, kg/ms.
μ_β β phase viscosity, kg/ms.
ρ_{air} ambient air density, kg/m^3.
ρ_g^0 saturated gas density, kg/m^3.
ρ_∞ ambient fluid density, kg/m^3.
ρ_g gas phase density, kg/m^3.
ρ_L liquid VOC phase density, kg/m^3.
ρ_β density of phase β, kg/m^3.
ρ_b soil dry bulk density, kg/m^3.
τ gas phase tortuosity.
ϕ porosity.
ω_s mass fraction of VOC in the solid phase.
$\omega_g^{(1)}$ mass fraction of VOC in the gas phase.
$\omega_g^{(2)}$ mass fraction of air in the gas phase.
$\omega_L^{(1)}$ mass fraction of VOC in the liquid VOC phase.
$\omega_L^{(2)}$ mass fraction of air in the liquid VOC phase.
$\omega_\beta^{(K)}$ mass fraction of component K in the β phase.

Acknowledgments. This work was supported by the Director, Office of Energy Research, Office of Basic Energy Sciences, Engineering, and Geosciences Division of the U.S. Department of Energy under contract DE-AC03-76SF00098. The authors would like to thank Chin Fu Tsang for his valuable contributions, and Marcelo Lippmann and Hoi-Ying Holman for reviewing this manuscript.

REFERENCES

Abriola, L. M., *Multiphase Migration of Organic Compounds in a Porous Medium*, Springer-Verlag, New York, 1984.

Abriola, L. M., and G. F. Pinder, A multiphase approach to the modelling of porous media contamination by organic compounds, 1, Equation development, *Water Resour. Res.*, *21*(1), 11–18, 1985*a*.

Abriola, L. M., and G. F. Pinder, A multiphase approach to the modelling of porous media contamination by organic compounds, 2, Numerical simulation, *Water Resour. Res.*, *21*(1), 19–26, 1985*b*.

Albertsen, M., and G. Matthes, Ground air measurement as a tool for mapping and evaluating organic groundwater pollution zones, paper presented at International Symposium on Groundwater Pollution by Oil Hydrocarbons, Int. Assoc. of Hydrol., Prague, 1978.

Baehr, A. L., Immiscible contaminant transport in soils with an emphasis on gasoline hydrocarbons, Ph.D. dissertation, Univ. of Delaware, Newark, 1984.

Baehr, A. L., Selective transport of hydrocarbons in the unsaturated zone due to aqueous and vapor phase partitioning, *Water Resour. Res.*, *23*(10), 1926–1938, 1987.

Baehr, A. L., and M. Y. Corapcioglu, A compositional multiphase model for groundwater contamination by petroleum products, 2, Numerical solution, *Water Resour. Res.*, *23*(1), 201–213, 1987.

Bear, J., *Hydraulics of Groundwater*, pp. 379–433, McGraw-Hill, New York, 1979.

Bejan, A., *Convection Heat Transfer*, John Wiley and Sons, New York, 1984.

Cheng, P., and W. J. Minkowycz, Free convection about a vertical flat plate embedded in a porous medium with application to heat transfer from a dike, *J. Geophys. Res.*, *82*(14), 2040–2044, 1977.

Devitt, D. A., R. B. Evans, W. A. Jury, T. H. Starks, B. Eklund, A. Sholsan, and J. J. Van Ee, *Soil Gas Sensing for Detection and Mapping of Volatile Organics*, U. S. Environmental Protection Agency, Las Vegas, Nev., 1987.

Fatt, I., and W. A. Klikoff, Effect of fractional wettability on multiphase flow through porous media, *AIME Trans.*, 216–246, 1959.

Freeze, R. A., and J. A. Cherry, *Groundwater*, pp. 403–404, Prentice-Hall, Princeton, N. J., 1979.

Hubbert, M. K., The theory of groundwater motion, *J. Geol.*, *48*(8), 785–944, 1940.

Hull, L. C., Soil gas surveying techniques and interpretation, paper presented at the In Situ Characterization and Monitoring Technique Workshop, Idaho Falls, Idaho, June 7–9, 1988.

Josephson, J., Subsurface organic contaminants, *Environ. Sci. Technol.*, *17*, 518*a*–521*a*, 1983.

Jury, W. A., W. F. Spencer, and W. J. Farmer, Behavior assessment model for trace organics in soil, I, Model description, *J. Environ. Qual.*, *12*(4), 558–564, 1983.

Jury, W. A., W. J. Farmer, and W. F. Spencer, Behavior assessment model for trace organics in soil, II, Chemical classification and parameter sensitivity, *J. Environ. Qual.*, *13*(4), 567–572, 1984*a*.

Jury, W. A., W. F. Spencer, and W. J. Farmer, Behavior assessment model for trace organics in soil, III, Application of screening model, *J. Environ. Qual.*, *13*(4), 573–579, 1984*b*.

Karickhoff, S. W., Semi-empirical estimation of sorption of hydrophobic pollutants on natural sediments and soils, *Chemosphere*, *10*(8), 833–846, 1981.

Karickhoff, S. W., D. S. Brown, and T. A. Scott, Sorption of hydrophobic pollutants on natural sediments, *Water Res.*, *13*, 241–248, 1979.

Lyman, W. J., W. F. Reehl, and D. H. Rosenblatt, *Handbook of Chemical Property Estimation Methods: Environmental Behavior of Organic Compounds*, McGraw-Hill, New York, 1982.

Marrin, D. L., and H. B. Kerfoot, Soil-gas surveying techniques, *Environ. Sci. Technol.*, *22*(7), 740–745, 1988.

Marrin, D. L., and G. M. Thompson, Gaseous behavior of TCE overlying a contaminated aquifer, *Groundwater*, *25*(1), 21–27, 1987.

Millington, R. J., and J. P. Quick, Permeability of porous solids, *Trans. Faraday Soc.*, *57*, 1200–1207, 1961.

Narasimhan, T. N., and P. A. Witherspoon, An integrated finite difference method for analyzing fluid flow in porous media, *Water Resour. Res.*, *12*(1), 57–64, 1976.

Pruess, K., TOUGH user's guide, Nucl. Regul. Comm., Rep. *NUREG/CR-4645*, Washington, D.C., June 1987.

Pruess, K., and J. S. Y. Wang, TOUGH-A numerical model for nonisothermal unsaturated flow to study waste canister heating effects, in *Materials Research Society Symposia Proceedings*, vol. 26, *Scientific Basis for Nuclear Waste Management*, edited by G. L. McVay, pp. 1031–1038, North-Holland, Amsterdam, 1984.

Reid, R. C., J. M. Prausnitz, and B. E. Poling, *The Properties of Gases and Liquids*, pp. 397–412, McGraw-Hill, New York, 1987.

Schwartzenbach, R. P., and J. Westfall, Transport of non-polar organic compounds from surface water to groundwater, Laboratory sorption studies, *Environ. Sci. Technol.*, *15*, 1360–1375, 1981.

Schwille, F., Migration of organic fluids immiscible with water, in *Pollutants in Porous Media, Ecological Studies no. 47*, pp. 27–48, Springer-Verlag, New York, 1984.

Silka, L. R., Simulation of vapor transport through the unsaturated zone—Interpretation of soil-gas surveys, *Groundwater Monit. Rev.*, *8*(2), 115–123, 1988.

Sleep, B. E., and J. F. Sykes, Modeling the transport of volatile organics in variably saturated media, *Water Resour. Res.*, *25*(1), 81–92, 1989.

Swallow, J. A., and P. M. Gschwend, Volatilization of organic compounds from unconfined aquifers, paper presented at the 3rd National Symposium on Aquifer Restoration and Groundwater Monitoring, Natl. Water Well Assoc., Columbus, Ohio, 1983.

Thompson, G. M., and D. L. Marrin, Soil gas contaminant investigations, a dynamic approach, *Groundwater Monit. Rev.*, 7, 88–93, 1987.

Tsang, Y. W., and K. Pruess, A study of thermally induced convection near a high-level nuclear waste repository in partially saturated fractured tuff, *Water Resour. Res.*, *23*(10), 1958–1966, 1987.

Wittman, S. G., K. J. Guinn, and R. D. Lee, Use of soil gas sampling techniques for assessment of groundwater contamination, paper presented at Proc. of Petrol. Hydrocarbons and Organic Chemicals in Groundwater, Natl. Water Well Assoc., Houston, Tex., 1985.

R. W. Falta, I. Javandel, K. Pruess, and P. A. Witherspoon, Earth Sciences Division, Lawrence Berkeley Laboratory, 1 Cyclotron Road, Berkeley, CA 94720.

(Received December 2, 1988;
revised June 6, 1989;
accepted June 26, 1989.)